

STABILITY OF FULLY DISCRETE LOCAL DISCONTINUOUS GALERKIN METHOD FOR THE GENERALIZED BENJAMIN-ONO EQUATION

MUKUL DWIVEDI AND TANMAY SARKAR

ABSTRACT. The main purpose of this paper is to design a fully discrete local discontinuous Galerkin (LDG) scheme for the generalized Benjamin-Ono equation. First, we analyze the stability for the semi-discrete LDG scheme and we prove that the scheme is L^2 -stable for general nonlinear flux. We develop a fully discrete LDG scheme using the Crank-Nicolson (CN) method and fourth-order fourth-stage Runge-Kutta (RK) method in time. Adapting the methodology established for the semi-discrete scheme, we demonstrate the stability of the fully discrete CN-LDG scheme for general nonlinear flux. Additionally, we consider the fourth-order RK-LDG scheme for higher order convergence in time and prove that it is strongly stable under an appropriate time step constraint by establishing a *three-step strong stability* estimate for linear flux. Numerical examples are provided to validate the efficiency and optimal order of accuracy for both the methods.

1. INTRODUCTION

We consider the following Cauchy problem associated to the Benjamin-Ono equation in the generalized form

$$\begin{cases} U_t + f(U)_x - \mathcal{H}U_{xx} = 0, & (x, t) \in \mathbb{R} \times (0, T], \\ U(x, 0) = U_0(x), & x \in \mathbb{R}, \end{cases} \quad (1.1)$$

where $T > 0$ is fixed, U_0 represents the prescribed initial data, f is the given flux function, and \mathcal{H} denotes the Hilbert transform [8, 23], defined by the principle value integral

$$\mathcal{H}U(x) := \text{P.V.} \frac{1}{\pi} \int_{\mathbb{R}} \frac{U(x-y)}{y} dy.$$

The Benjamin-Ono equation (1.1) is a nonlinear, non-local partial differential equation that finds application in various physical phenomena [17]. In particular, the propagation of weakly nonlinear internal long waves in a fluid with a thin region of stratification can be represented by the Benjamin-Ono equation. Originating from the modeling of waves in shallow water, it offers insights into the behavior of these waves, including their propagation and interaction. Furthermore, we mention that it defines a Hamiltonian system, and with the help of inverse scattering method (see [1]), families of localized solitary wave solutions, called as soliton solutions [5], can be obtained under the appropriate assumptions on the initial data. Since the Benjamin-Ono equation is completely integrable, it admits infinitely many conserved quantities [5].

The investigation into the well-posedness of the Cauchy problem (1.1) associated to the Benjamin-Ono equation has been the subject of extensive research over the years. Pioneering work in the local well-posedness was conducted by Iório [16] for the initial data in $H^s(\mathbb{R})$, $s > 3/2$ and making use of the conserved quantities, the global well-posedness for data in $H^s(\mathbb{R})$, $s \geq 2$ is demonstrated. Tao

(Mukul Dwivedi)

DEPARTMENT OF MATHEMATICS, INDIAN INSTITUTE OF TECHNOLOGY JAMMU, JAGTI, NH-44 BYPASS ROAD, POST OFFICE NAGROTA, JAMMU - 181221, INDIA

(Tanmay Sarkar)

DEPARTMENT OF MATHEMATICS, INDIAN INSTITUTE OF TECHNOLOGY JAMMU, JAGTI, NH-44 BYPASS ROAD, POST OFFICE NAGROTA, JAMMU - 181221, INDIA

E-mail addresses: 2020rma1031@iitjammu.ac.in, tanmay.sarkar@iitjammu.ac.in.

2020 Mathematics Subject Classification. Primary: 65M60, 35R09; Secondary: 65M12.

Key words and phrases. Local discontinuous Galerkin method, Benjamin-Ono equation, Hilbert transform, stability.

in [22] also obtained the global well-posedness in $H^1(\mathbb{R})$ by introducing the Gauge transformation. The idea of Gauge transformation given in [22] was further improved by Kenig et al. [15] to carry out the local well-posedness to $H^s(\mathbb{R})$ for $s \geq 0$. Molinet [19] has also obtained the global well-posedness for the periodic data in $L^2(\mathbb{R})$.

It is well-known that due to the effects of dispersion and nonlinear convection, finding a reliable method for the Benjamin-Ono equation is quite challenging task. Nevertheless, recent decades have seen the development of various numerical methods to solve the equation (1.1), with only the pertinent literature referenced here. An implicit finite difference method introduced by Thomée et al. [23] utilizes the continuous Hilbert transform. More recently, Dutta et al. [8] demonstrated the convergence of the fully discrete finite difference scheme, which includes the discrete Hilbert transform, and Galtung [12] devised a convergent Crank-Nicolson Galerkin scheme.

The discontinuous Galerkin (DG) method, a finite element approach, was first introduced by Reed and Hill [20] for the neutron transport equation. It was later extended by Cockburn et al. to tackle nonlinear conservation laws effectively, as detailed in [6]. However, DG methods face challenges with equations containing higher-order derivatives, which can introduce instability and inconsistency, as noted by Hesthaven [13]. To address this, Bassi and Rebay [3] adapted the DG method, introducing the Runge-Kutta DG (RKDG) variant for compressible Navier-Stokes equations. Cockburn and Shu further generalized this approach in their local discontinuous Galerkin (LDG) method [7], designed specifically for higher-order problems. LDG transforms equations into first-order systems by introducing auxiliary variables, which approximate lower derivatives. The “local” nature of LDG allows these auxiliary variables to be eliminated locally, enabling stable and efficient numerical flux design at interfaces. Thus, LDG addresses higher-order derivatives in a way that ensures stability and accurate solutions.

The LDG method has been developed to deal with equations that have higher-order derivative terms. For instance, Yan and Shu [28] devised a LDG method for KdV type equations, which have third-order spatial derivatives. Furthermore, Xu and Shu [27] expanded the LDG method to handle equations with fourth and fifth order spatial derivatives.

In more recent times, the LDG method has become popular for dealing with partial differential equations that involve the non-local operator. Xu and Hesthaven [25] came up with an LDG method that breaks down the fractional Laplacian of order α ($1 < \alpha < 2$) into second-order derivatives and fractional integrals of order $2 - \alpha$. Similarly, Aboelenen [2] and Dwivedi et al. [11] developed a LDG method specifically designed for fractional Schrödinger-type equations and fractional Korteweg-de Vries equation respectively.

Research on developing fully discrete LDG schemes with stability analysis for equations involving higher-order derivatives without diffusion is quite limited. Recent advancements have introduced a stable fully discrete LDG method known as the high-order RK-LDG method. Various studies have investigated the stability of this method in various contexts, as seen in [21]. Recently, Hunter et al. [14] determined the stability of a fully discrete implicit-explicit RK method for the linearized KdV equation with periodic initial data using the Fourier method. However, to the best of our knowledge, the LDG method has not been developed for the Benjamin-Ono equation.

In this paper, our approach to design the LDG scheme for the Benjamin-Ono equation (1.1) involves introduction of auxiliary variables to represent (1.1) into the system with lower order derivatives. A crucial part of this process involves constructing appropriate numerical fluxes at the interior interfaces, while boundary numerical fluxes are determined by the prescribed boundary conditions. Additionally, to develop a fully discrete LDG scheme, we discretize time using the Crank-Nicolson method. We demonstrate that the fully discrete scheme is stable for any general nonlinear flux. The main ingredients of the paper are enlisted below:

- (1) We design a LDG scheme for the Benjamin-Ono equation (1.1) and establish the stability of the devised semi-discrete scheme with a general nonlinear flux. The stability analysis has also been extended for fully discrete Crank-Nicolson scheme.
- (2) Furthermore, we extend our methodology to include higher order temporal discretization of equation (1.1) using the classical four-stage fourth-order Runge-Kutta (RK) method

[21]. For the linear case, we are able to show that the proposed fully discrete scheme is *strongly stable* through the *two-step* and *three-step strong stability* estimates.

- (3) We demonstrate the rates obtained by numerical illustrations are optimal and it preserves the conserved quantity like mass and momentum in discrete set up.

The rest of the paper is organized as follows. We commence our investigation by introducing a few preliminary lemmas and semi-discrete LDG scheme and its stability analysis in Section 2. We present the stability analysis of the fully discrete Crank-Nicolson LDG scheme for general nonlinear flux and fully discrete fourth-order RK-LDG scheme for linear flux in Section 3. The efficiency of the scheme is validated through some numerical examples presented in Section 4. Concluding remarks and a few remarks about future work are given in Section 5.

2. SEMI-DISCRETE LDG SCHEME

2.1. Preliminary results. Hereby we describe a few relevant properties of the Hilbert transform through the following lemma. It is worthwhile to mention that these properties are instrumental for subsequent analysis. Let $\mathcal{S}(\mathbb{R})$ denotes the Schwartz space.

Lemma 2.1. (See [18, Chapter 15]) *Let $\phi \in \mathcal{S}(\mathbb{R})$. Then the Hilbert transform \mathcal{H} satisfies the following properties:*

i) *Skew symmetric:*

$$(\mathcal{H}\phi_1, \phi_2) = -(\phi_1, \mathcal{H}\phi_2), \quad \forall \phi_1, \phi_2 \in L^2(\mathbb{R}).$$

ii) *Commutates with derivatives:*

$$\mathcal{H}\phi_x = (\mathcal{H}\phi)_x.$$

iii) *L^2 -isometry property:*

$$\|\mathcal{H}\phi\|_{L^2(\mathbb{R})} = \|\phi\|_{L^2(\mathbb{R})}.$$

iv) *Orthogonality:*

$$(\mathcal{H}\phi, \phi) = 0.$$

where (\cdot, \cdot) is the standard L^2 -inner product.

Given that the original problem is defined over the entire real line due to the involvement of a non-local operator \mathcal{H} . However, for the numerical purpose, following the similar approach in [25, 23], we restrict it to a sufficiently large bounded domain $\Omega := [a, b]$, where $a < b$, such that U has a compact support within Ω for all time $0 < t < T$. Hence it becomes imperative to impose the boundary conditions: $U(a, t) = 0 = U(b, t)$, for all $t < T$. Moreover, the properties of the Hilbert transform introduced in the Lemma 2.1 remain applicable for a bounded domain Ω , provided ϕ has a compact support within Ω .

We partition the domain Ω into intervals $I_i = (x_{i-\frac{1}{2}}, x_{i+\frac{1}{2}})$ with $a = x_{\frac{1}{2}} < x_{\frac{3}{2}} < \dots < x_{N+\frac{1}{2}} = b$, where N represents the number of elements. This partition creates a mesh of elements denoted by \mathcal{I} , with each element having a spatial step size $h_i = x_{i+\frac{1}{2}} - x_{i-\frac{1}{2}}$ and a maximum step size $h = \max_{1 \leq i \leq N} \{h_i\}$. In conjunction with this mesh, we define the broken Sobolev spaces as follows:

$$H^1(\Omega, \mathcal{I}) := \{v : \Omega \rightarrow \mathbb{R} \mid v|_{I_i} \in H^1(I_i), i = 1, 2, \dots, N\};$$

and

$$L^2(\Omega, \mathcal{I}) := \{v : \Omega \rightarrow \mathbb{R} \mid v|_{I_i} \in L^2(I_i), i = 1, 2, \dots, N\}.$$

Within this framework, we introduce the notation $v_{i+\frac{1}{2}}$ to represent the value of v at the nodes $\{x_{i+\frac{1}{2}}\}$, and denote the one-sided limits as

$$v_{i+\frac{1}{2}}^\pm = v(x_{i+\frac{1}{2}}^\pm) := \lim_{x \rightarrow x_{i+\frac{1}{2}}^\pm} v(x).$$

We define the local inner product and local $L^2(I_i)$ norm as follows:

$$(u, v)_{I_i} = \int_{I_i} uv \, dx, \quad \|u\|_{I_i} = (u, u)_{I_i}^{\frac{1}{2}}, \quad (u, v) = \sum_{i=1}^N (u, v)_{I_i} \quad \text{and} \quad \|u\|_{L^2(\Omega)} = \sum_{i=1}^N \|u\|_{I_i}.$$

With all these preparation we introduce the auxiliary variables P and Q such that

$$P = \mathcal{H}Q, \quad Q = U_x.$$

As a consequence, the equation (1.1) can be represented in the following equivalent form of first order differential system

$$\begin{aligned} U_t &= -(f(U) - P)_x, \\ P &= \mathcal{H}Q, \\ Q &= U_x. \end{aligned} \tag{2.1}$$

Prior to introducing the LDG scheme, we assume that the exact solution (U, P, Q) of the system (2.1) belongs to

$$\mathcal{T}_3 \times K(\Omega, \mathcal{I}) := H^1(0, T; H^1(\Omega, \mathcal{I})) \times L^2(0, T; H^1(\Omega, \mathcal{I})) \times L^2(0, T; L^2(\Omega, \mathcal{I})).$$

This implies that the solution (U, P, Q) of (2.1) satisfies the following system:

$$\begin{aligned} (U_t, v)_{I_i} &= (f(U) - P, v_x)_{I_i} - (fv - Pv) \Big|_{x_{i-\frac{1}{2}}^+}^{x_{i+\frac{1}{2}}^-}, \\ (P, w)_{I_i} &= (\mathcal{H}Q, w)_{I_i}, \\ (Q, z)_{I_i} &= -(U, z_x)_{I_i} + (Uz) \Big|_{x_{i-\frac{1}{2}}^+}^{x_{i+\frac{1}{2}}^-}, \end{aligned} \tag{2.2}$$

for all $w \in L^2(\Omega, \mathcal{I})$, $v, z \in H^1(\Omega, \mathcal{I})$, and for $i = 1, 2, \dots, N$.

We define the finite element $V^k \subset H^1(\Omega, \mathcal{I})$ by

$$V^k = \{v \in L^2(\Omega) : v|_{I_i} \in P^k(I_i), \forall i = 1, 2, \dots, N\}, \tag{2.3}$$

where $P^k(I_i)$ is space of polynomials of degree up to order k (≥ 1) on I_i .

2.2. LDG scheme. To develop the LDG scheme for the Benjamin-Ono equation, it is necessary to define the numerical fluxes \hat{u} , \hat{p} and the nonlinear flux \hat{f} at interfaces and boundaries. We introduce the following notations:

$$\{\{u\}\} = \frac{u^- + u^+}{2}, \quad \llbracket u \rrbracket = u^+ - u^-.$$

We choose the alternative numerical flux which is given by

$$\hat{p} = p^+, \quad \hat{u} = u^-, \tag{2.4}$$

or alternatively,

$$\hat{p} = p^-, \quad \hat{u} = u^+,$$

at interface $x_{i+\frac{1}{2}}$, $i = 1, 2, \dots, N-1$. We set the boundary flux as

$$\begin{aligned} \hat{u}_{N+\frac{1}{2}} &= U(b, t) = 0, \quad \hat{u}_{\frac{1}{2}} = U(a, t) = 0, \quad \text{for all } t < T, \\ \hat{p}_{N+\frac{1}{2}} &= p_{N+\frac{1}{2}}^-, \quad \hat{p}_{\frac{1}{2}} = p_{\frac{1}{2}}^+. \end{aligned} \tag{2.5}$$

For the nonlinear flux \hat{f} , we can use any consistent and monotone flux [28]. In particular, we consider the following Lax-Friedrichs flux

$$\hat{f} = \hat{f}(u^-, u^+) = \frac{1}{2}(f(u^-) + f(u^+) - \delta \llbracket u \rrbracket), \quad \delta = \max_u |f'(u)|, \tag{2.6}$$

where the maximum is taken over a range of u in a relevant element.

Applying the DG approach in all the equations of the above system (2.2), we design the scheme as follows: we seek an approximations

$$(u, p, q) \in H^1(0, T; V^k) \times L^2(0, T; V^k) \times L^2(0, T; V^k) =: \mathcal{T}_3 \times \mathcal{V}^k$$

to (U, P, Q) , where U is an exact solution of (1.1) with $P = \mathcal{H}Q$, $Q = U_x$, such that for all test functions $(v, w, z) \in \mathcal{T}_3 \times \mathcal{V}^k$ and $i = 1, \dots, N$, the following system of equations holds:

$$\begin{aligned} (u_t, v)_{I_i} &= (f(u) - p, v_x)_{I_i} - \left(\hat{f}v - \hat{p}v \right) \Big|_{x_{i-\frac{1}{2}}^+}^{x_{i+\frac{1}{2}}^-}, \\ (p, w)_{I_i} &= (\mathcal{H}q, w)_{I_i}, \\ (q, z)_{I_i} &= -(u, z_x)_{I_i} + (\hat{u}z) \Big|_{x_{i-\frac{1}{2}}^+}^{x_{i+\frac{1}{2}}^-}, \\ (u^0, v)_{I_i} &= (U_0, v)_{I_i}. \end{aligned}$$

The above system of equations can be rewritten as

$$\begin{aligned} (u_t, v)_{I_i} &= \mathcal{F}_i(f(u), v) - \mathcal{D}_i^+(p, v), \\ (p, w)_{I_i} &= (\mathcal{H}q, w)_{I_i}, \\ (q, z)_{I_i} &= -\mathcal{D}_i^-(u, z), \\ (u^0, v)_{I_i} &= (U_0, v)_{I_i}, \end{aligned} \tag{2.7}$$

where

$$\begin{aligned} \mathcal{F}_i(f(u), v) &= (f(u), v_x)_{I_i} - \hat{f}_{i+\frac{1}{2}} v_{i+\frac{1}{2}}^- + \hat{f}_{i-\frac{1}{2}} v_{i-\frac{1}{2}}^+, \quad \text{for } i = 1, 2, \dots, N, \\ \mathcal{D}_i^+(p, v) &= (p, v_x)_{I_i} - p_{i+\frac{1}{2}}^+ v_{i+\frac{1}{2}}^- + p_{i-\frac{1}{2}}^+ v_{i-\frac{1}{2}}^+, \quad \text{for } i = 1, 2, \dots, N-1, \\ \mathcal{D}_i^-(u, z) &= (u, z_x)_{I_i} - u_{i+\frac{1}{2}}^- v_{i+\frac{1}{2}}^- + u_{i-\frac{1}{2}}^- v_{i-\frac{1}{2}}^+, \quad \text{for } i = 2, 3, \dots, N-1, \end{aligned}$$

and

$$\begin{aligned} \mathcal{D}_1^-(u, z) &= (u, z_x)_{I_1} - u_{\frac{3}{2}}^- v_{\frac{3}{2}}^-, \quad \mathcal{D}_N^-(u, z) = (u, z_x)_{I_N} + u_{N-\frac{1}{2}}^- v_{N-\frac{1}{2}}^+, \\ \mathcal{D}_N^+(p, v) &= (p, v_x)_{I_N} - p_{N+\frac{1}{2}}^- v_{N+\frac{1}{2}}^- + p_{N-\frac{1}{2}}^+ v_{N-\frac{1}{2}}^+. \end{aligned}$$

The proposed LDG scheme (2.7) for the Benjamin-Ono equation works in the following way: given u , we use the third equation of (2.7) to obtain q locally; more precisely, q in the cell I_i can be computed with the information of u in the cells I_{i-1} and I_i . Afterwards, with the help of q in the cell I_i , one can obtain p locally in the cell I_i . Finally, we update the approximate solution u in the cell I_i incorporating p and u in the cells I_{i-1} and I_i . In a similar way, for the choice of alternative fluxes $\hat{p} = p^-$, $\hat{u} = u^+$ the algorithm can be adopted accordingly.

Summing equation (2.7) over $i = 1, 2, \dots, N$, we have

$$\begin{aligned} (u_t, v) &= \mathcal{F}(f(u), v) + \mathcal{D}^+(p, v), \\ (p, w) &= (\mathcal{H}q, w), \\ (q, z) &= \mathcal{D}^-(u, z), \end{aligned} \tag{2.8}$$

where

$$\mathcal{F} = \sum_{i=1}^N \mathcal{F}_i \quad \text{and} \quad \mathcal{D}^\pm = - \sum_{i=1}^N \mathcal{D}_i^\pm.$$

Consequently, we represent \mathcal{F} , \mathcal{D}^\pm and associated numerical fluxes in the following way:

$$\mathcal{F}(f(u), v) = \sum_{i=1}^N (f(u), v_x)_{I_i} - \sum_{i=1}^N (\hat{f}v) \Big|_{x_{i-\frac{1}{2}}^+}^{x_{i+\frac{1}{2}}^-} = (f(u), v_x) + \hat{f}_{\frac{1}{2}} v_{\frac{1}{2}}^+ - \hat{f}_{N+\frac{1}{2}} v_{N+\frac{1}{2}}^- + \sum_{i=1}^{N-1} \hat{f}_{i+\frac{1}{2}} \llbracket v \rrbracket_{i+\frac{1}{2}}, \tag{2.9}$$

$$\mathcal{D}^+(p, v) = -(p, v_x) - p_{\frac{1}{2}}^+ v_{\frac{1}{2}}^+ + p_{N+\frac{1}{2}}^- v_{N+\frac{1}{2}}^- - \sum_{i=1}^{N-1} p_{i+\frac{1}{2}}^+ \llbracket v \rrbracket_{i+\frac{1}{2}}, \tag{2.10}$$

and similarly,

$$\mathcal{D}^-(u, z) = -(u, z_x) - \sum_{i=1}^{N-1} u_{i+\frac{1}{2}}^- \llbracket z \rrbracket_{i+\frac{1}{2}}. \quad (2.11)$$

Moreover, we have the following result.

Proposition 2.2. *Let u and $p \in V^k$. Then, we have*

$$\mathcal{D}^+(p, u) + \mathcal{D}^-(u, p) = 0. \quad (2.12)$$

Proof. We observe that integration by parts yields the following

$$\begin{aligned} (p, u_x) + (u, p_x) &= \sum_{i=1}^N ((p, u_x)_{I_i} + (u, p_x)_{I_i}) = \sum_{i=1}^N (up) \Big|_{x_{i-\frac{1}{2}}^+}^{x_{i+\frac{1}{2}}^-} \\ &= -u_{\frac{1}{2}}^+ p_{\frac{1}{2}}^+ + u_{N+\frac{1}{2}}^- p_{N+\frac{1}{2}}^- - \sum_{i=1}^{N-1} u_{i+\frac{1}{2}}^- \llbracket p \rrbracket_{i+\frac{1}{2}} - \sum_{i=1}^{N-1} p_{i+\frac{1}{2}}^+ \llbracket u \rrbracket_{i+\frac{1}{2}}. \end{aligned}$$

From (2.10) and (2.11), we have

$$\begin{aligned} \mathcal{D}^+(p, u) + \mathcal{D}^-(u, p) &= -(p, u_x) - (u, p_x) - p_{\frac{1}{2}}^+ u_{\frac{1}{2}}^+ + p_{N+\frac{1}{2}}^- u_{N+\frac{1}{2}}^- - \sum_{i=1}^{N-1} p_{i+\frac{1}{2}}^+ \llbracket u \rrbracket_{i+\frac{1}{2}} \\ &\quad - \sum_{i=1}^{N-1} u_{i+\frac{1}{2}}^- \llbracket p \rrbracket_{i+\frac{1}{2}} = 0. \end{aligned}$$

Hence the result follows. \square

To carry out the further analysis of the LDG scheme (2.7), we define the corresponding compact form

$$\begin{aligned} \mathcal{B}(u, p, q; v, w, z) &= \sum_{i=1}^N \left[(u_t, v)_{I_i} + (p, w)_{I_i} - (\mathcal{H}q, w)_{I_i} + (q, z)_{I_i} \right] \\ &\quad - \mathcal{F}(f(u), v) - \mathcal{D}^+(p, v) - \mathcal{D}^-(u, z), \end{aligned} \quad (2.13)$$

for all $(u, p, q) \in \mathcal{T}_3 \times K(\Omega, \mathcal{I})$ and $(v, w, z) \in \mathcal{T}_3 \times \mathcal{V}^k$.

Hereby we analyze the stability the proposed semi-discrete LDG scheme (2.7) for (1.1).

2.3. Stability of semi-discrete scheme. We prove the following stability lemma for general flux function using an appropriate compact form:

Lemma 2.3. (*L^2 -stability*) *Let u, p, q be obtained from the LDG scheme (2.7). Then the LDG scheme (2.7) for Benjamin-Ono equation (1.1) is L^2 -stable. We have the following estimate*

$$\|u(\cdot, T)\|_{L^2(\Omega)} \leq C \|u^0\|_{L^2(\Omega)}, \quad (2.14)$$

for any $T > 0$ and a constant C .

Proof. Since we have the compact form (2.13) of the scheme (2.7), we choose the test functions $(v, w, z) = (u, -q, p)$ in (2.13), which yields

$$\begin{aligned} \mathcal{B}(u, p, q; u, -q, p) &= \sum_{i=1}^N \left[(u_t, u)_{I_i} - (p, q)_{I_i} + (\mathcal{H}q, q)_{I_i} + (q, p)_{I_i} \right] \\ &\quad - \mathcal{F}(f(u), u) - \mathcal{D}^+(p, u) - \mathcal{D}^-(u, p). \end{aligned} \quad (2.15)$$

Using the Proposition 2.2, estimate (2.9) and result from Lemma 2.1 in (2.15), we have

$$\mathcal{B}(u, p, q; u, -q, p) = (u_t, u) - \sum_{i=1}^N (f(u), u_x)_{I_i} - \hat{f}_{\frac{1}{2}} u_{\frac{1}{2}}^+ + \hat{f}_{N+\frac{1}{2}} u_{N+\frac{1}{2}}^- - \sum_{i=1}^{N-1} \hat{f}_{i+\frac{1}{2}} \llbracket u \rrbracket_{i+\frac{1}{2}}. \quad (2.16)$$

Let us define $F(u) = \int^u f(u) du$. Then we have

$$\sum_{i=1}^N (f(u), u_x)_{I_i} = \sum_{i=1}^N F(u) \Big|_{u_{i-\frac{1}{2}}^+}^{u_{i+\frac{1}{2}}^-} = - \sum_{i=1}^{N-1} \llbracket F(u) \rrbracket_{i+\frac{1}{2}} - F(u)_{\frac{1}{2}} + F(u)_{N+\frac{1}{2}}. \quad (2.17)$$

Incorporating (2.17) in equation (2.16), we have

$$\begin{aligned} \mathcal{B}(u, p, q; u, -q, p) &= (u_t, u) + \sum_{i=1}^{N-1} \llbracket F(u) \rrbracket_{i+\frac{1}{2}} + F(u)_{\frac{1}{2}} - F(u)_{N+\frac{1}{2}} \\ &\quad - \hat{f}_{\frac{1}{2}} u_{\frac{1}{2}}^+ + \hat{f}_{N+\frac{1}{2}} u_{N+\frac{1}{2}}^- - \sum_{i=1}^{N-1} \hat{f}_{i+\frac{1}{2}} \llbracket u \rrbracket_{i+\frac{1}{2}}. \end{aligned} \quad (2.18)$$

Since (u, p, q) satisfies the LDG scheme (2.7), then we have

$$\mathcal{B}(u, p, q; v, w, z) = 0,$$

for any $(v, w, z) \in V^k$. As a result, we get

$$\begin{aligned} (u_t, u)_{L^2(\Omega)} + \sum_{i=1}^{N-1} \llbracket F(u) \rrbracket_{i+\frac{1}{2}} + F(u)_{\frac{1}{2}} - F(u)_{N+\frac{1}{2}} \\ - \hat{f}_{\frac{1}{2}} u_{\frac{1}{2}}^+ + \hat{f}_{N+\frac{1}{2}} u_{N+\frac{1}{2}}^- - \sum_{i=1}^{N-1} \hat{f}_{i+\frac{1}{2}} \llbracket u \rrbracket_{i+\frac{1}{2}} = 0. \end{aligned} \quad (2.19)$$

Since the numerical flux $\hat{f} = \hat{f}(u^-, u^+)$ is monotone, it is non-decreasing in its first argument and non-increasing in its second argument. As a consequence, we have

$$\llbracket F(u) \rrbracket_{i+\frac{1}{2}} - \hat{f}_{i+\frac{1}{2}} \llbracket u \rrbracket_{i+\frac{1}{2}} > 0,$$

for all $i = 1, 2, \dots, N-1$. Dropping the positive term from left-hand side of equation (2.18) and using the boundary conditions, we end up with

$$\frac{1}{2} \frac{d}{dt} \|u\|_{L^2(\Omega)}^2 \leq 0. \quad (2.20)$$

Applying the Gronwall's inequality, we obtain

$$\|u(\cdot, T)\|_{L^2(\Omega)} \leq C \|u^0\|_{L^2(\Omega)}.$$

Hence the result follows. \square

3. STABILITY OF FULLY DISCRETE LDG SCHEME

3.1. Stability analysis of Crank-Nicolson fully discrete LDG scheme. To develop the fully discrete local discontinuous Galerkin (LDG) scheme, we utilize the Crank-Nicolson method for time discretization in (2.8). We partition the time domain using a time step τ . Let $\{t_n = n\tau\}_{n=0}^M$ be the partition of the given time interval $[0, T]$, and define $u^n = u(t_n)$ and $u^{n+\frac{1}{2}} = \frac{u^{n+1} + u^n}{2}$.

The fully discrete LDG scheme is designed as follows: Given u^n find u^{n+1} such that the following system holds

$$\begin{aligned} (u^{n+1}, v) &= (u^n, v) + \tau \mathcal{F}(f(u^{n+\frac{1}{2}}), v) + \tau \mathcal{D}^+(p^n, v), \\ (p^n, w) &= (\mathcal{H}q^n, w), \\ (q^n, z) &= \mathcal{D}^-(u^{n+\frac{1}{2}}, z), \end{aligned} \quad (3.1)$$

for all $v, w, z \in V^k$ and $n = 1, 2, \dots, M-1$, and set $u^0 = \mathcal{P}^- u_0$. Numerical fluxes at interfaces and boundaries involved in the above scheme can be defined in a similar way as in (2.4)-(2.6).

Lemma 3.1. *The fully discrete scheme (3.1) is L^2 -stable, and the solution u^n obtained by the scheme (3.1) satisfies*

$$\|u^{n+1}\|_{L^2(\Omega)} \leq \|u^n\|_{L^2(\Omega)}, \quad \forall n. \quad (3.2)$$

Proof. We choose test functions $(v, w, z) = (u^{n+\frac{1}{2}}, -q^n, p^n)$ in (3.1), and adding all three equations yields

$$\begin{aligned} \left(\frac{u^{n+1} - u^n}{\tau}, u^{n+\frac{1}{2}} \right) &= \mathcal{F}(f(u^{n+\frac{1}{2}}), u^{n+\frac{1}{2}}) + \mathcal{D}^+(p^n, u^{n+\frac{1}{2}}) + (p^n, q^n) - (\mathcal{H}q^n, q^n) \\ &\quad - (q^n, p^n) + \mathcal{D}^-(u^{n+\frac{1}{2}}, p^n). \end{aligned}$$

Using Lemma 2.1, Proposition 2.2 and monotonicity of the numerical flux $\hat{f}^{n+\frac{1}{2}}$ in the above equation, we obtain

$$\left(\frac{u^{n+1} - u^n}{\tau}, u^{n+\frac{1}{2}} \right) \leq 0.$$

This implies

$$\|u^{n+1}\|_{L^2(\Omega)} \leq \|u^n\|_{L^2(\Omega)}, \quad \forall n = 0, 1, \dots, M-1.$$

This completes the proof. \square

3.2. Stability analysis of higher order fully discrete LDG scheme. Hereby we focus on the stability analysis with an explicit fourth-order Runge-Kutta time discretization. The spatial stability of LDG schemes are demonstrated in Section 2. It is worth mentioning that the stability analysis under the higher-order time discretizations is a challenging task, and at present we have pursued this analysis exclusively in the linear case. In particular, for simplicity, we choose the zero flux function for the subsequent analysis [24]. We would like to remark that to the best of our knowledge, the stability analysis for fourth-order LDG schemes involving general LDG operators has not been performed in the literature. The following analysis can be considered as a contribution to the stability analysis under the aforementioned assumptions.

Then the semi-discrete scheme (2.7) corresponds to an ODE system

$$\frac{d}{dt}u = L_h u. \quad (3.3)$$

where LDG operator L_h can be recovered from the semi-discrete scheme (2.7). We consider the four-stage explicit fourth-order RK method for time discretization [21]:

$$u^{n+1} = P_4(\tau L_h)u^n, \quad (3.4)$$

where the operator P_4 is given by

$$P_4(\tau L_h) = I + \tau L_h + \frac{1}{2}(\tau L_h)^2 + \frac{1}{6}(\tau L_h)^3 + \frac{1}{24}(\tau L_h)^4.$$

We introduce a few notations which will be used frequently in subsequent stability analysis. We say that the LDG operator L_h is semi-negative if $(v, (L_h + L_h^T)v) \leq 0, \forall v \in V^k$ and it is denoted by $L_h + L_h^T \leq 0$. We define $[u, v] := -(u, (L_h + L_h^T)v)$. It is a bilinear form on V^k . For convenience, we denote $\mathcal{L}_h := \tau L_h$. We introduce the notion of strong stability for the fully discrete scheme.

Definition 3.2 (Strong stability). *Let u^n be the approximate solution obtained by the fully discrete scheme (3.4). Then the scheme (3.4) is said to be strongly stable if there exists an integer n_0 , such that*

$$\|u^n\|_{L^2(\Omega)} \leq \|u^0\|_{L^2(\Omega)}, \quad \forall n \geq n_0. \quad (3.5)$$

Hereby we state the following result associated to energy estimate which will be instrumental for further stability analysis.

Lemma 3.3 (Energy equality [21]). *Let u^n be the solution of fully discrete scheme (3.4). Then*

$$\|u^{n+1}\|_{L^2(\Omega)}^2 - \|u^n\|_{L^2(\Omega)}^2 = \mathcal{Q}(u^n), \quad \forall n \geq 1,$$

where

$$\mathcal{Q}(u^n) = \frac{1}{576} \|\mathcal{L}_h^4 u^n\|_{L^2(\Omega)}^2 - \frac{1}{72} \|\mathcal{L}_h^3 u^n\|_{L^2(\Omega)}^2 + \tau \sum_{i,j=0}^3 \alpha_{ij} [\mathcal{L}_h^i u^n, \mathcal{L}_h^j u^n],$$

and

$$A = (\alpha_{ij})_{i,j=0}^3 = - \begin{pmatrix} 1 & 1/2 & 1/6 & 1/24 \\ 1/2 & 1/3 & 1/8 & 1/24 \\ 1/6 & 1/8 & 1/24 & 1/48 \\ 1/24 & 1/24 & 1/48 & 1/144 \end{pmatrix}.$$

In Lemma 3.3, $\mathcal{Q}(u^n)$ is referred as the energy change of the approximate solution, consisting of two components: the numerical dissipation $\frac{1}{576} \|\mathcal{L}_h^4 u^n\|_{L^2(\Omega)}^2 - \frac{1}{72} \|\mathcal{L}_h^3 u^n\|_{L^2(\Omega)}^2$ and the quadratic form $\tau \sum_{i,j=0}^3 \alpha_{ij} [\mathcal{L}_h^i u^n, \mathcal{L}_h^j u^n]$. The next lemma establishes the negativity of the quadratic form, also provides conditions for the strong stability.

Lemma 3.4 (See Lemma 2.4 in [21]). *Let L_h be a semi-negative operator and*

$$\mathcal{Q}_1(u) = \zeta \|\mathcal{L}_h^3(u)\|_{L^2(\Omega)} + \tau \sum_{i,j=0}^m \bar{\alpha}_{ij} [\mathcal{L}_h^i u, \mathcal{L}_h^j u], \quad (3.6)$$

where $\bar{\alpha}_{ij} = \bar{\alpha}_{ji}$ and $m \geq 2$. If $\zeta < 0$ and $\bar{A} = (\bar{\alpha}_{ij})_{i,j=0}^m$ is negative definite, then there exists a constant $c_0 > 0$ such that $\mathcal{Q}_1(u) \leq 0$ provided $\|L_h\| \leq c_0$, where c_0 is independent of τ and h .

For simplicity, we are using uniform time stepping. Since the semi-discrete scheme (2.7) is spatially stable from the Lemma 2.3, that is

$$\left(\frac{d}{dt} u, u \right) = (L_h u, u) \leq 0,$$

the LDG operator L_h is semi-negative by the following

$$\left(\frac{d}{dt} u, u \right) = (L_h u, u) = \frac{1}{2} (L_h u, u) + \frac{1}{2} (u, L_h u) = \frac{1}{2} ((L_h + L_h^T) u, u) \leq 0,$$

implies $L_h + L_h^T \leq 0$.

The question of whether the classical fourth-order Runge-Kutta method is strongly stable or not remained open until Sun and Shu partially addressed it in [21], where they provided a counterexample showing that this method is not always strongly stable for semi-negative operators. However, it is worth noting that the semi-negative operator provided in the counterexample in [21] is not a DG operator. We introduce a new approach to demonstrate the strong stability of the fourth-order, four-stage RK-LDG scheme (3.4). By proving stability of the fully discrete scheme over two and three time steps, we establish the foundation from which the strong stability result follows. More precisely, we prove the following:

Theorem 3.5. *Let $L_h + L_h^T \leq 0$. Then the four-stage fourth-order RK LDG scheme (3.4) is strongly stable. That is, we have*

$$\|u^n\|_{L^2(\Omega)} \leq \|u^0\|_{L^2(\Omega)}, \quad \forall n \geq 2,$$

provided $\tau \|L_h\| \leq c_0$, where c_0 is a constant.

Before proceeding with the proof of Theorem 3.5, we establish the three-step strong stability result.

Proposition 3.6 (Three-step strong stability). *Let $L_h + L_h^T \leq 0$. Then the four-stage fourth-order RK scheme (3.4) is strongly stable in three steps. Therefore, we have*

$$\|u^{n+3}\|_{L^2(\Omega)} \leq \|u^n\|_{L^2(\Omega)}, \quad n \geq 0, \quad (3.7)$$

provided $\tau \|L_h\| \leq c_0$, where c_0 is a constant.

Proof. From the Lemma 3.3, energy equality implies

$$\|u^{n+3}\|_{L^2(\Omega)}^2 - \|u^n\|_{L^2(\Omega)}^2 = \mathcal{Q}(u^{n+2}) + \mathcal{Q}(u^{n+1}) + \mathcal{Q}(u^n), \quad (3.8)$$

where $\mathcal{Q}(u^n)$ is defined in Lemma 3.3. We find the estimates for $\mathcal{Q}(u^{n+1})$ and $\mathcal{Q}(u^{n+2})$ in terms of u^n in its quadratic part by the following calculation:

$$\begin{aligned}\mathcal{Q}(u^{n+1}) &= \frac{1}{576} \|\mathcal{L}_h^4 u^{n+1}\|_{L^2(\Omega)}^2 - \frac{1}{72} \|\mathcal{L}_h^3 u^{n+1}\|_{L^2(\Omega)}^2 + \tau \sum_{i,j=0}^3 \alpha_{ij} [\mathcal{L}_h^i u^{n+1}, \mathcal{L}_h^j u^{n+1}] \\ &= \frac{1}{576} \|\mathcal{L}_h^4 u^{n+1}\|_{L^2(\Omega)}^2 - \frac{1}{72} \|\mathcal{L}_h^3 u^{n+1}\|_{L^2(\Omega)}^2 + \tau \sum_{i,j=0}^3 \alpha_{ij} [\mathcal{L}_h^i P_4(\mathcal{L}_h) u^n, \mathcal{L}_h^j P_4(\mathcal{L}_h) u^n] \\ &= \frac{1}{576} \|\mathcal{L}_h^4 u^{n+1}\|_{L^2(\Omega)}^2 - \frac{1}{72} \|\mathcal{L}_h^3 u^{n+1}\|_{L^2(\Omega)}^2 + \tau \sum_{i,j=0}^7 \tilde{\alpha}_{ij} [\mathcal{L}_h^i u^n, \mathcal{L}_h^j u^n]\end{aligned}$$

We define the matrices A_0 and A_1 as

$$A_0 = (\alpha_{ij})_{i,j=0}^3 = - \begin{pmatrix} 1 & 1/2 & 1/6 \\ 1/2 & 1/3 & 1/8 \\ 1/6 & 1/8 & 1/24 \end{pmatrix}, \quad A_1 = (\tilde{\alpha}_{ij})_{i,j=0}^7 = - \begin{pmatrix} 1 & 3/2 & 7/6 \\ 3/2 & 7/3 & 15/8 \\ 7/6 & 15/8 & 37/24 \end{pmatrix}.$$

Our interest in the first 3×3 coefficient matrix as it is important to note that this is sufficient to apply the result in Lemma 3.4. While the complete matrix can be obtained and is not difficult, it involves a lengthy derivation. For brevity, we choose not to provide the complete matrix here, and we refer to [21] for detailed information.

In a similar way, we obtain

$$\begin{aligned}\mathcal{Q}(u^{n+2}) &= \frac{1}{576} \|\mathcal{L}_h^4 u^{n+2}\|_{L^2(\Omega)}^2 - \frac{1}{72} \|\mathcal{L}_h^3 u^{n+2}\|_{L^2(\Omega)}^2 + \tau \sum_{i,j=0}^3 \alpha_{ij} [\mathcal{L}_h^i u^{n+2}, \mathcal{L}_h^j u^{n+2}] \\ &= \frac{1}{576} \|\mathcal{L}_h^4 u^{n+2}\|_{L^2(\Omega)}^2 - \frac{1}{72} \|\mathcal{L}_h^3 u^{n+2}\|_{L^2(\Omega)}^2 + \tau \sum_{i,j=0}^7 \tilde{\alpha}_{ij} [\mathcal{L}_h^i u^{n+1}, \mathcal{L}_h^j u^{n+1}] \\ &= \frac{1}{576} \|\mathcal{L}_h^4 u^{n+2}\|_{L^2(\Omega)}^2 - \frac{1}{72} \|\mathcal{L}_h^3 u^{n+2}\|_{L^2(\Omega)}^2 + \tau \sum_{i,j=0}^7 \tilde{\alpha}_{ij} [\mathcal{L}_h^i P_4(\mathcal{L}_h) u^n, \mathcal{L}_h^j P_4(\mathcal{L}_h) u^n] \\ &= \frac{1}{576} \|\mathcal{L}_h^4 u^{n+2}\|_{L^2(\Omega)}^2 - \frac{1}{72} \|\mathcal{L}_h^3 u^{n+2}\|_{L^2(\Omega)}^2 + \tau \sum_{i,j=0}^{11} \hat{\alpha}_{ij} [\mathcal{L}_h^i u^n, \mathcal{L}_h^j u^n],\end{aligned}$$

where

$$A_2 = (\hat{\alpha}_{ij})_{i,j=0}^{11} = - \begin{pmatrix} 1 & 5/2 & 19/6 \\ 5/2 & 19/3 & 57/8 \\ 19/6 & 57/8 & 253/24 \end{pmatrix}.$$

Assuming $\|\mathcal{L}_h\| \leq 2$, we have the following estimates

$$\begin{aligned}\frac{1}{576} \|\mathcal{L}_h^4 u^{n+2}\|_{L^2(\Omega)}^2 - \frac{1}{72} \|\mathcal{L}_h^3 u^{n+2}\|_{L^2(\Omega)}^2 &\leq 0, \\ \frac{1}{576} \|\mathcal{L}_h^4 u^{n+1}\|_{L^2(\Omega)}^2 - \frac{1}{72} \|\mathcal{L}_h^3 u^{n+1}\|_{L^2(\Omega)}^2 &\leq 0, \\ \frac{1}{576} \|\mathcal{L}_h^4 u^n\|_{L^2(\Omega)}^2 - \frac{1}{72} \|\mathcal{L}_h^3 u^n\|_{L^2(\Omega)}^2 &\leq -\frac{1}{144} \|\mathcal{L}_h^3 u^n\|_{L^2(\Omega)}^2.\end{aligned}$$

Hence (3.8) becomes

$$\|u^{n+3}\|_{L^2(\Omega)}^2 - \|u^n\|_{L^2(\Omega)}^2 \leq -\frac{1}{144} \|\mathcal{L}_h^3 u^n\|_{L^2(\Omega)}^2 + \tau \sum_{i,j=0}^{11} \bar{\alpha}_{ij} [\mathcal{L}_h^i u^n, \mathcal{L}_h^j u^n] =: \mathcal{Q}_1(u^n).$$

Afterwards, we define the matrix A as

$$A := (\bar{\alpha}_{ij})_{i,j=0}^{11} = (\alpha_{ij})_{i,j=0}^3 + (\tilde{\alpha}_{ij})_{i,j=0}^7 + (\hat{\alpha}_{ij})_{i,j=0}^{11} = - \begin{pmatrix} 3 & 9/2 & 9/2 \\ 9/2 & 9 & 73/8 \\ 9/2 & 73/8 & 97/8 \end{pmatrix}.$$

Since the eigenvalues of A are -21.9444 , -1.64399 and -0.536623 , it follows that A is negative definite. Applying the Lemma 3.4, we obtain $\mathcal{Q}_1(u^n) \leq 0$. As a consequence, we have

$$\|u^{n+3}\|_{L^2(\Omega)} \leq \|u^n\|_{L^2(\Omega)}.$$

Hence the result follows. \square

Proof of Theorem 3.5. Since the LDG operator is semi-negative, applying the two-step stability result from [21, Theorem 2.1], we have

$$\|u^{n+2}\|_{L^2(\Omega)} \leq \|u^n\|_{L^2(\Omega)}, \quad (3.9)$$

provided $\tau \|L_h\| \leq c_0$, where c_0 is a constant. The estimate (3.9) along with the estimate (3.7) combined together provide the desired stability estimate of the fully discrete LDG scheme (3.4). \square

4. NUMERICAL EXPERIMENTS

In this section, our goal is to validate the proposed LDG scheme (2.7) for the Benjamin-Ono equation (1.1). We begin our numerical validation using the Crank-Nicolson (CN) LDG scheme (3.1) with $\tau = 0.5h$ and $k = 1$. We employ the periodic one soliton solution of the Benjamin-Ono equation. It is important to note that since the implicit term appears in the nonlinear part of the scheme (3.1), we use the Newton iteration to solve it at each time step.

Rate of convergence R_E for errors is defined for each intermediate step between element numbers N_1 and N_2 as

$$R_E = \frac{\ln(E(N_1)) - \ln(E(N_2))}{\ln(N_2) - \ln(N_1)},$$

where E is a function of number of elements N and represents the L^2 -error. The Benjamin-Ono equation (1.1) possesses an infinite number of conserved quantities [12]. Hereby we consider the first two specific quantities known as *mass* and *momentum*. With normalization, these quantities in the discrete set up can be expressed as follows:

$$\mathbf{C}_1^h := \frac{\int_{\Omega} u \, dx}{\int_{\Omega} U_0 \, dx}, \quad \mathbf{C}_2^h := \frac{\|u\|_{L^2(\Omega)}}{\|U_0\|_{L^2(\Omega)}}.$$

Our aim is to preserve these quantities in the discrete set up.

We compare approximate solution u obtained by (3.1) with the exact periodic solution of the Benjamin-Ono equation (1.1) with $f(U) = \frac{1}{2}U^2$. For instance, we consider the solution of (1.1) from Thomée et. al. [23] (also see [9, 10])

$$U(x, t) = \frac{2c\delta}{1 - \sqrt{1 - \delta^2} \cos(c\delta(x - ct))}, \quad \delta = \frac{\pi}{cL}, \quad (4.1)$$

where we choose $L = 15$, $c = 0.25$. We compare the above exact solution at the final time $T = 20$. This solution characterizes periodic solitary waves, exhibiting periodicity and amplitude determined by the parameters L and c respectively. Table 4.2 presents the L^2 -errors of the proposed fully discrete CN-LDG scheme (3.1) using a polynomial of degree one. The results confirm that the numerically obtained rates are optimal and that the approximate solution u converges to the exact solution U .

To achieve the higher order accuracy of the proposed LDG scheme, we perform the numerical results using the four-stage fourth-order explicit Runge-Kutta LDG scheme (3.4) of

$$U_t = -\frac{1}{2}(U^2)_x + \mathcal{H}U_{xx}. \quad (4.2)$$

Our focus lies on verifying the performance of the scheme using a low storage explicit Runge-Kutta (LSERK) of fourth-order time discretization [4, 11, 13] of the form

$$\begin{aligned} y^{(0)} &= u_h^n, \\ k^0 &= 0, \\ \text{for } j &= 1 : 5 \end{aligned}$$

N	E	R_E	\mathbf{C}_1^h	\mathbf{C}_2^h
160	1.65e-02		1.04	0.97
		2.14		
320	3.77e-03		1.05	0.97
		2.07		
640	8.98e-04		1.02	0.98
		2.04		
1280	2.18e-04		1.00	1.00

TABLE 4.1. L^2 -error and rate of convergence R_E for the CN-LDG scheme at time $T = 20$ taking N elements and polynomial degree $k = 1$.

$$\begin{cases} k^j = a_j k^{j-1} + \tau L_h y^{(j-1)}, \\ y^{(j)} = y^{(j-1)} + b_j k^j, \end{cases}$$

$$u_h^{n+1} = y^{(5)},$$

where the weighted coefficients a_j , b_j and c_j of the LSERK method given in [13]. The above defined iteration is equivalent to the classical fourth-order method (3.4) [13]. LSERK is considerably more efficient and accurate than (3.4) since it has the disadvantage that it requires four extra storage arrays. We are providing the steps of algorithm to compute the approximate solution using LDG scheme (2.7) with LSERK time discretization, for more details one may refer to [13].

Algorithm 1 Numerical Procedure for Benjamin-Ono Equation

- 1: Set up problem parameters and initial conditions
 - 2: Compute time step size dt based on CFL condition
 - 3: Determine total number of time steps $Nsteps$ based on Final time and dt
 - 4: **for** $tstep = 1$ to $Nsteps$ **do**
 - 5: **for** $INTRK = 1$ to 5 **do**
 - 6: Compute local time $timelocal$ for current stage
 - 7: Evaluate right-hand side Lu of the differential equation using Algorithm 2
 - 8: Update solution u using Runge-Kutta stages
 - 9: **end for**
 - 10: Increment time by dt
 - 11: **end for**
 - 12: **return** Final solution u
-

Algorithm 2 Algorithm for Computing RHS of equation (4.2)

Require: Solution u , left boundary value xL , right boundary value xR , current time $timelocal$

Ensure: Right-hand side of the equation $rhsu$

- 1: Compute coefficients and variables based on initial conditions and boundary values
 - 2: Define field differences at interfaces, including boundary conditions
 - 3: Compute flux for u
 - 4: Compute local variable q and its differences using u
 - 5: Compute local variable p , using Hilbert transform of q
 - 6: Compute flux for p ($fluxp$)
 - 7: Compute squared differences of u , du^2 at interfaces, and impose boundary conditions
 - 8: Compute flux for the convective term ($fluxf$)
 - 9: Compute derivative of the flux ($dfdr$)
 - 10: Compute right-hand side of the semi-discrete PDE ($rhsu$)
 - 11: **return** $rhsu$
-

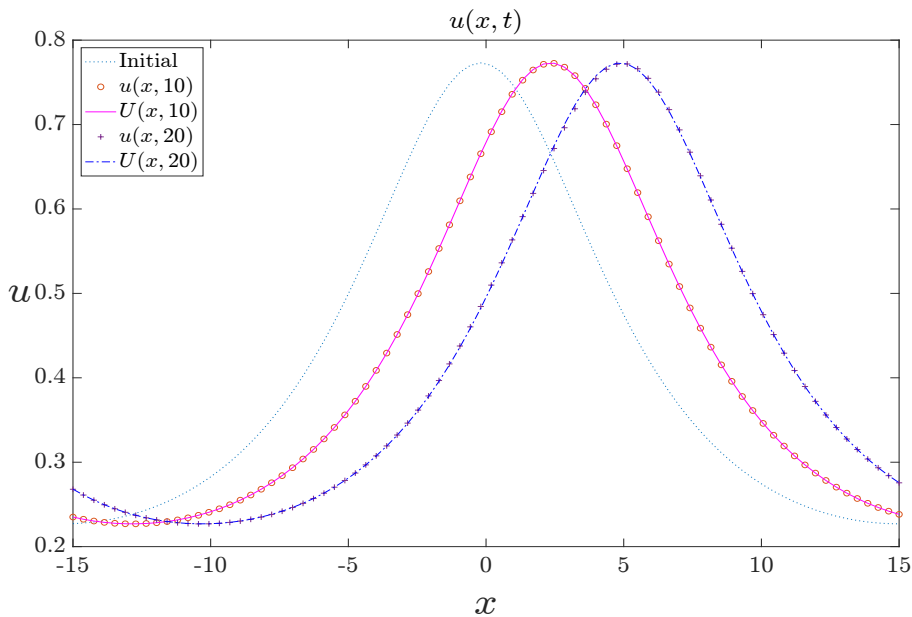


FIGURE 4.1. Exact $U(x, t)$ and approximate solution $u(x, t)$ computed by the RK-LDG scheme at $T = 10$ and $T = 20$ with $N = 160$, $k = 3$ and initial condition $U(x, 0)$ of (1.1).

In numerical implementation with LSERK time discretization, we initially compare the approximate solution obtained from the LDG scheme (2.7) with the exact solution (4.1) at time $t = 10$, and further at the final time $t = 20$. Figure 4.1 depicts the comparison of the solution at various times. This validation confirms that the numerical scheme converges to the exact solution. The Table 4.2 presents the L^2 -errors of the proposed scheme under polynomial degree up to three. It is observed that the errors are converging to zero with relatively coarser grids and optimal orders of convergence are obtained at time $T = 10$ for each polynomial degree up to three and the discrete conserved quantities C_1^h and C_2^h are also preserved. Similar analysis has been carried out at time $T = 20$ and details are presented in Table 4.3 and optimal rates are obtained there as well.

We have also approached to compute the approximation of the Hilbert transform by using the Gaussian quadrature for other soliton solutions [12, 23]. However, we do not achieve the optimal rates or the theoretical rates obtained by convergence analysis. Similar observations are also described in [12, Section 5]. One possible interpretation is that the principal value integral is not being computed accurately near the singularity, and it is most likely caused by our approximation of the full line problem by restricting to a bounded interval while still employing the full line Hilbert transform.

5. CONCLUDING REMARKS

We have designed a local discontinuous Galerkin method for the Benjamin-Ono equation with general nonlinear flux. We have shown that the semi-discrete scheme is stable. The stability analysis is also carried out for the fully discrete Crank-Nicolson LDG scheme considering any general nonlinear flux function and strong stability of fourth-order Runge-Kutta LDG scheme under certain assumptions on the flux function. The theoretical convergence analysis for fully discrete scheme incorporating fourth-order Runge-Kutta time marching scheme involving general nonlinear flux will be addressed in the future work. In the numerical experiments, it is observed that the L^2 -error is quite small even for the coarser grids and the optimal rates are obtained for various degrees of polynomials which demonstrates the efficiency and accuracy of the proposed scheme. In addition, the proposed fully discrete schemes preserve the conservative quantities such as mass and momentum.

k	$k = 1$		$k = 2$		$k = 3$			
	E	R_E	E	R_E	E	R_E	\mathbf{C}_1^h	\mathbf{C}_2^h
40	2.91e-01		3.65e-02		8.69e-03		1.01	1.01
		2.01		2.76		4.37		
80	7.15e-02		5.37e-03		4.20e-04		1.00	1.00
		2.02		2.93		4.07		
160	1.77e-02		7.029e-04		2.49e-05		1.00	1.00
		2.00		2.98		4.00		
320	4.40e-03		8.88e-05		1.56e-06		1.00	1.00

TABLE 4.2. L^2 -error and rate of convergence R_E for the RK-LDG scheme at time $T = 10$ taking N elements and polynomial degree k with normalized conserved quantities \mathbf{C}_1^h and \mathbf{C}_2^h .

k	$k = 1$		$k = 2$		$k = 3$			
	E	R_E	E	R_E	E	R_E	\mathbf{C}_1^h	\mathbf{C}_2^h
40	6.02e-01		6.015e-01		5.98e-02		0.99	0.98
		2.05		2.65		4.46		
80	1.45e-01		9.54e-02		2.718e-03		1.00	1.00
		2.02		2.90		4.09		
160	3.56e-02		1.27e-02		1.59e-04		1.00	1.00
		2.01		2.97		4.02		
320	8.83e-03		1.62e-03		9.80e-06		1.00	1.00

TABLE 4.3. L^2 -error and rate of convergence R_E for the RK-LDG scheme at time $T = 20$ taking N elements and polynomial degree k with normalized conserved quantities \mathbf{C}_1^h and \mathbf{C}_2^h .

CONFLICTS OF INTEREST

The authors declare that they have no known competing financial interests that could have appeared to influence the work reported in this paper. Furthermore, no data was used for the research described in the article.

REFERENCES

- [1] M. J. Ablowitz and A. S. Fokas. The inverse scattering transform for the Benjamin-Ono equation—a pivot to multidimensional problems. *Studies in Applied Mathematics*, 68 (1983), no. 1, 1–10.
- [2] T. Aboelenen. A high-order nodal discontinuous Galerkin method for nonlinear fractional Schrödinger type equations. *Communications in Nonlinear Science and Numerical Simulation*, 54 (2018), 428–452.
- [3] F. Bassi and S. Rebay. A high-order accurate discontinuous finite element method for the numerical solution of the compressible Navier–Stokes equations. *Journal of Computational Physics*, 131 (1997), no. 2, 267–279.
- [4] H. M. Carpenter and A. C. Kennedy. Fourth-order 2N-storage Runge-Kutta schemes. *NASA TM 109112*, NASA Langley Research Center, 1994.
- [5] K. M. Case. Benjamin-Ono related equations and their solutions. *Proceedings of the National Academy of Sciences*, 76 (1979), no. 1, 1–3.
- [6] B. Cockburn, G. E. Karniadakis and C.-W. Shu. Discontinuous Galerkin methods: theory, computation and applications. *Springer Science & Business Media*, 2012.
- [7] B. Cockburn and C.-W. Shu. The local discontinuous Galerkin method for time-dependent convection-diffusion systems. *SIAM Journal on Numerical Analysis*, 35 (1998), no. 6, 2440–2463.
- [8] R. Dutta, H. Holden, U. Koley and N. H. Risebro. Convergence of finite difference schemes for the Benjamin-Ono equation. *Numerische Mathematik*, 134 (2016), no. 2, 249–274.
- [9] M. Dwivedi and T. Sarkar. Stability and convergence analysis of a Crank-Nicolson Galerkin scheme for the fractional Korteweg-de Vries equation. *SMAI Journal of Computational Mathematics*, 10 (2024), 107–139.
- [10] M. Dwivedi and T. Sarkar. Fully discrete finite difference schemes for the fractional Korteweg-de Vries equation. *Journal of Scientific Computing*, 101 (2024), no. 30.
- [11] M. Dwivedi and T. Sarkar. Local discontinuous Galerkin method for fractional Korteweg-de Vries equation. *arXiv preprint arXiv:2404.18069*, (2024).

- [12] S. T. Galtung. Convergent Crank–Nicolson Galerkin scheme for the Benjamin-Ono equation. *Discrete and Continuous Dynamical Systems*, 38 (2018), no. 3, 1243–1268.
- [13] J. S. Hesthaven and T. Warburton. Nodal discontinuous Galerkin methods: algorithms, analysis, and applications. *Springer Science and Business Media*, 2007.
- [14] J. Hunter, Z. Sun and Y. Xing. Stability and time-Step constraints of implicit-explicit Runge-Kutta methods for the linearized Korteweg-de Vries equation. *Communications on Applied Mathematics and Computation*, 6 (2024), no. 1, 658–687.
- [15] A. Ionescu and C. E. Kenig. Global well-posedness of the Benjamin-Ono equation in low-regularity spaces. *Journal of the American Mathematical Society*, 20 (2007), no. 3, 753–798.
- [16] R. J. Iório. On the Cauchy problem for the Benjamin-Ono equation. *Communications in Partial Differential Equations*, 11 (1986), no. 10, 1031–1081.
- [17] Y. Ishimori. Solitons in a one-dimensional Lennard-Jones lattice. *Progress of Theoretical Physics*, 68 (1982), no. 2, 402–410.
- [18] F. W. King. Hilbert transforms: Volume 2. *Cambridge University Press*, 2009.
- [19] L. Molinet. Global well-posedness in L^2 for the periodic Benjamin-Ono equation. *American Journal of Mathematics*, 130 (2008), no. 3, 635–683.
- [20] W. H. Reed and T. R. Hill. Triangular mesh methods for the neutron transport equation. *Technical Report LA-UR-73-479, Los Alamos Scientific Lab*, 1973.
- [21] Z. Sun and C.-W. Shu. Stability of the fourth-order Runge-Kutta method for time-dependent partial differential equations. *Annals of Mathematical Sciences and Applications*, 2 (2017), no. 2, 255–284.
- [22] T. Tao. Global well-posedness of the Benjamin-Ono equation in $H^1(\mathbb{R})$. *Journal of Hyperbolic Differential Equations*, 1 (2004), no. 1, 27–49.
- [23] V. Thomée and A. S. V. Murthy. A numerical method for the Benjamin-Ono equation. *BIT Numerical Mathematics*, 38 (1998), 597–611.
- [24] H. Wang, Q. Tao, C.-W. Shu, and Q. Zhang. Analysis of Local Discontinuous Galerkin Methods with Implicit-Explicit Time Marching for Linearized KdV Equations. *SIAM Journal on Numerical Analysis*, 62 (2024), no. 5, 2222–2248.
- [25] Q. Xu and J. S. Hesthaven. Discontinuous Galerkin method for fractional convection-diffusion equations. *SIAM Journal on Numerical Analysis*, 52 (2014), no. 1, 405–423.
- [26] Y. Xu, Q. Zhang, C.-W. Shu and H. wang. The L^2 -norm stability analysis of Runge-Kutta discontinuous Galerkin methods for linear hyperbolic equations. *SIAM Journal on Numerical Analysis*, 57 (2019), no. 4, 1574–1601.
- [27] Y. Xu and C.-W. Shu. Local discontinuous Galerkin methods for high-order time-dependent partial differential equations. *Communications in Computational Physics*, 7 (2010), no. 1, 1–46.
- [28] J. Yan and C.-W. Shu. A local discontinuous Galerkin method for KdV type equations. *SIAM Journal on Numerical Analysis*, 40 (2002), no. 2, 769–791.